

Arc dacite genesis pathways: Evidence from mafic enclaves and their hosts in Aegean lavas

G.F. Zellmer^{a,b,*}, S.P. Turner^c

^a Institute of Earth Sciences, Academia Sinica, 128 Academia Road, Section 2, Nankang, Taipei 11529, Taiwan, ROC

^b Lamont-Doherty Earth Observatory, 61 Route 9W, Palisades, New York 10964, USA

^c GEMOC, Department of Earth and Planetary Sciences, Macquarie University, Sydney, NSW 2109, Australia

Received 4 January 2006; accepted 17 August 2006

Available online 25 September 2006

Abstract

Mafic enclaves are commonly found in intermediate arc magmas, and their occurrence has been linked to eruption triggering by pre-eruptive magma mixing processes. New major, trace, Sr–Nd and U–Th isotope data of rocks from Nisyros in the Aegean volcanic arc are presented here. Pre-caldera samples display major and trace element trends that are consistent with fractionation of magnetite and apatite within intermediate compositions, and zircon within felsic compositions, and preclude extensive hybridization between mafic and felsic magmas. In contrast, post-caldera dacites form a mixing trend towards their mafic enclaves. In terms of U-series isotopes, most samples show small ²³⁸U excesses of up to ~10%. Mafic enclaves have significantly higher U/Th ratios than their dacitic host lavas, precluding simple models that relate the mafic and felsic magmas by fractionation or aging alone. A more complicated petrogenetic scenario is required. The post-caldera dacites are interpreted to represent material remobilized from a young igneous protolith following influx of fresh mafic magma, consistent with the U–Th data and with Sr–Nd isotope constraints that point to very limited (<10%) assimilation of old crust at Nisyros. When these results are compared to data from Santorini in the same arc, there are many geochemical similarities between the two volcanic centers during the petrogenesis of the pre-caldera samples. However, striking differences are apparent for the post-caldera lavas: in Nisyros, dacites show geochemical and textural evidence for magma mixing and remobilization by influx of mafic melts, and they erupt as viscous lava domes; in Santorini, evidence for geochemical hybridization of dacites and mafic enclaves is weak, dacite petrogenesis does not involve protolith remobilization, and lavas erupt as less viscous flows. Despite these differences, it appears that mafic enclaves in intermediate Aegean arc magmas consistently yield timescales of at least 100 kyrs between U enrichment of the mantle wedge and eruption, on the upper end of those estimated for the eruptive products of mafic arc volcanoes. Finally, the data presented here provide constraints on the rates of differentiation from primitive arc basalts to dacites (less than ~140 kyrs), and on the crustal residence time of evolved igneous protoliths prior to their remobilization by mafic arc magmas (greater than ~350 kyrs).

© 2006 Elsevier B.V. All rights reserved.

Keywords: Mafic enclaves; Remobilization; U-series isotopes; Timescales; Petrogenesis

1. Introduction

A variety of processes have been identified as potential triggering mechanisms for volcanic eruptions, including volatile build-up, fractional crystallization and

* Corresponding author. Institute of Earth Sciences, Academia Sinica, 128 Academia Road, Section 2, Nankang, Taipei 11529, Taiwan, ROC. Tel.: +886 2 2783 9910x602; fax: +886 2 2783 9871.

E-mail address: gzellmer@earth.sinica.edu.tw (G.F. Zellmer).

magma recharge (e.g. Francis et al., 2000). In particular, it has been shown that the injection of mafic magma into a magma reservoir of intermediate composition may trigger eruption due to the combined effects of increased mass, heat and volatile input (Sparks et al., 1977). The abundance of mafic enclaves in andesites and dacites from a number of arc volcanoes, and disequilibrium textures in the host lavas, provide support for this model (e.g., Bacon, 1986; Clynne, 1999; Murphy et al., 2000; Harford and Sparks, 2001; Zellmer et al., 2003b; Mortazavi and Sparks, 2004). However, the petrogenetic relationship between mafic enclaves and their host lavas remains elusive, and the origin of arc lavas of intermediate composition is still controversial (e.g., Reagan et al., 2003; Zellmer et al., 2003a, 2005).

U–Th isotopes provide information on time scales of <350 kyrs and can, in principle, be used to determine the age relationships between different magmas (e.g., Condomines et al., 2003; Turner et al., 2003). In the simplest model, island arc dacites evolve largely by fractional crystallization from basaltic parents, which typically have ^{238}U excesses. Since ^{238}U excesses return to secular equilibrium via ^{230}Th in-growth, mafic enclaves injected prior to eruption into a dacite produced by fractionation of similar but older basalts should plot vertically below the dacite at lower $(^{230}\text{Th}/^{232}\text{Th})$ on a U–Th equiline diagram (Fig. 1a). However, it has been suggested that some arc dacites are produced by a more complex process involving a combination of partial remelting of older arc basalts and partial crystallization of new mafic inputs in a lower crustal hot-zone (Annen and Sparks, 2002). So long as the process only involves remelting of previous arc inputs, a similar relationship should result in U–Th isotope space because old lavas will have simply evolved vertically up to the equiline (Fig. 1b). In contrast, assimilation of old continental crust with low U/Th ratios will result in a trajectory to low $(^{230}\text{Th}/^{232}\text{Th})$ and U/Th (Fig. 1c). Thus, in combination with other geochemical and petrological data, U–Th isotopes may provide valuable constraints on different models for the origin of, and the relationships between, mafic and evolved arc magmas.

In this contribution, data from lavas erupted on Nisyros in the Aegean volcanic arc, including a number of dacites and associated mafic enclaves, are presented. Together with data from Santorini (Zellmer et al., 2000), which also include a number of dacites and mafic enclaves, the results are then used to explore likely relationships between the mafic and evolved compositions, and to provide constraints on the processes and rates of petrogenetic evolution of intermediate arc magmas.

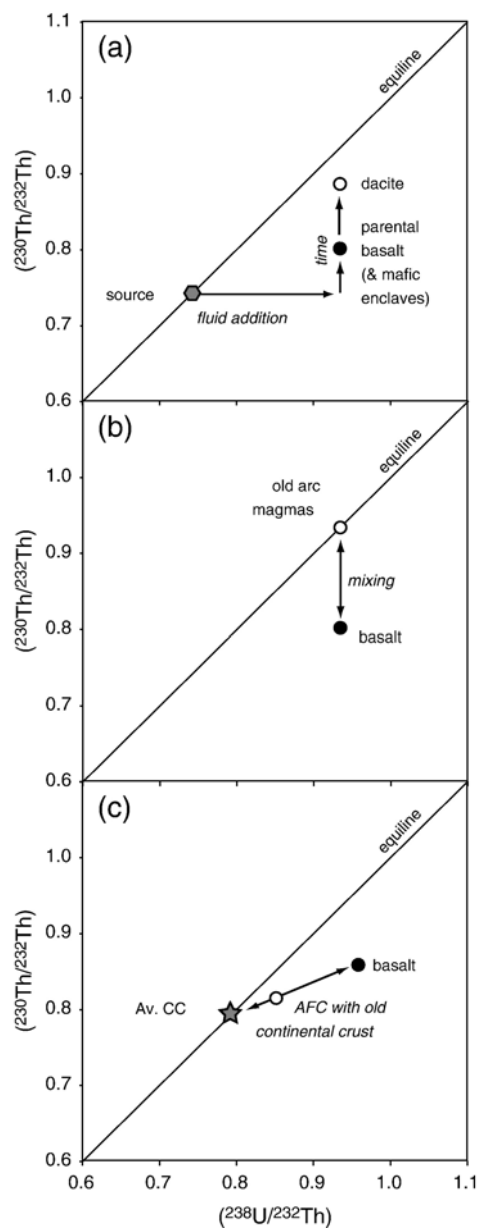


Fig. 1. The U–Th equiline diagram can be used to test simple models for the petrogenesis of intermediate arc magmas and their mafic enclaves. (a) In arcs, the U–Th mantle wedge composition is dominated by subducted sediments, e.g. GLOSS (Plank and Langmuir, 1998). Fluid addition to the mantle wedge produces ^{238}U excesses in the parental basalts. Dacites are generated through fractional crystallization from these basalts over time, resulting in a vertical array. (b) A similar array is produced by mixing of basalts with more evolved arc magmas that formed as in (a), but aged to secular equilibrium. (c) Mixing of basalts with old continental crust, e.g. average CC (Taylor and McLennan, 1995), will also produce dacites, but will introduce a range in U/Th ratios.

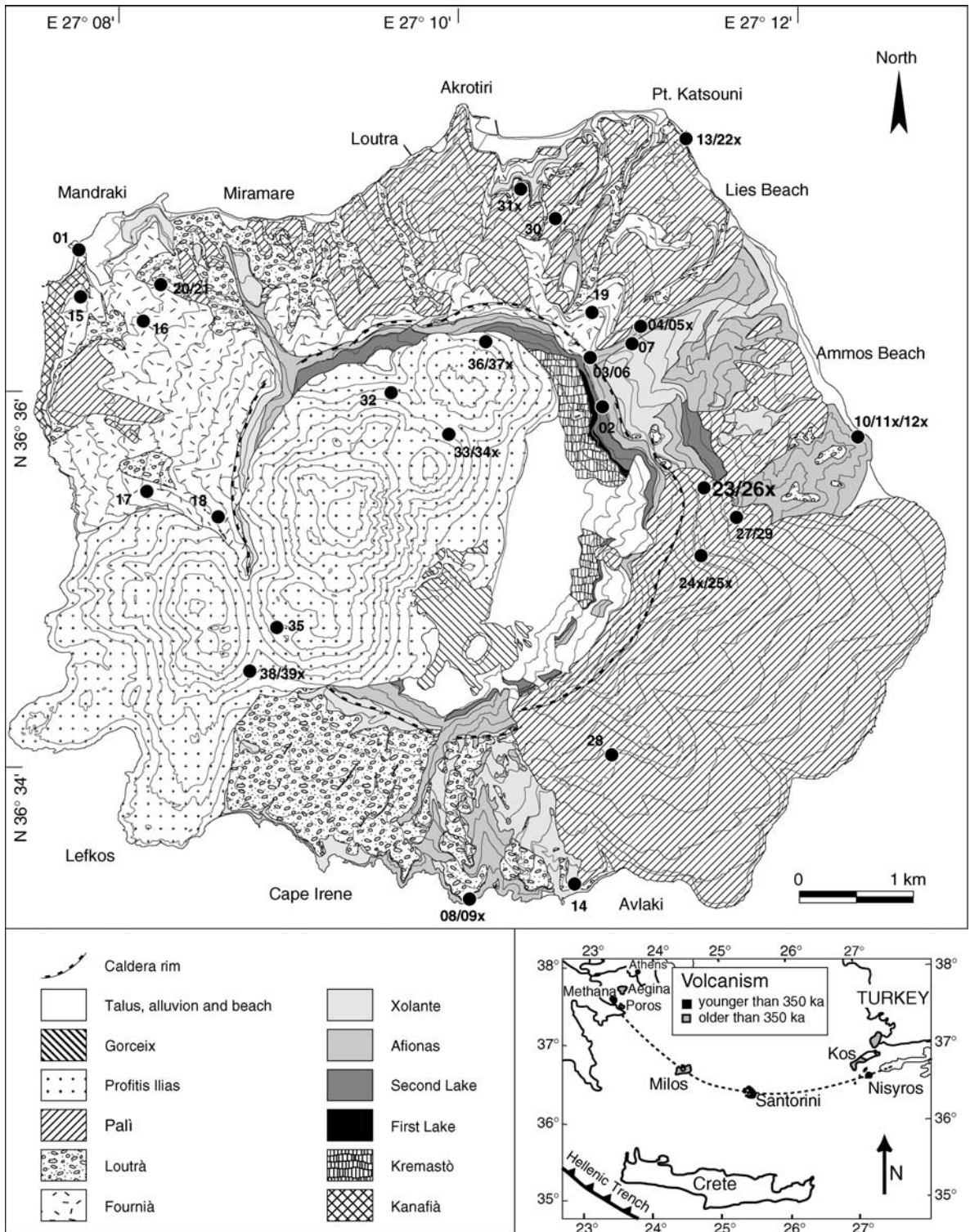


Fig. 2. Outline geological map of Nisyros, adapted from Volentik et al. (2005a). Sampling locations and GZNI sample numbers are indicated (cf. Tables 1–3). Inset: Map of the Aegean volcanic arc, with sites of young volcanic activity in black. Nisyros is the easternmost site of active volcanism.

2. Geological background

The island of Nisyros is situated at 36°35' N/27°11' E, and is the easternmost volcano of the active Aegean arc (see inset to Fig. 2). A simplified geological map of Nisyros, adapted from Volentik et al. (2005a), is given in Fig. 2, and sample locations are indicated. The detailed stratigraphy and the volcanological evolution of the island are discussed in Volentik et al. (2005b) and Vanderkluysen et al. (2005), and are briefly summarized here. The volcanic history began with a transition from sub-marine to subaerial eruptions less than ~160 kyrs ago, followed by a complex history of volcanic construction and sporadic destruction, leading to the formation of a stratocone composed of basaltic andesitic to rhyolitic lava flows, and pyroclastic and debris avalanche deposits. Eruption of the Pali synthem of rhyolitic lava flows and white pumices then resulted in the formation of the present caldera. Subsequent magmatic activity involved the partial filling of this caldera through effusion of six voluminous lava domes (Profitis Ilias synthem), here referred to as the post-caldera dacites.

There are very few radiometric eruption age constraints for Nisyros. The absence of K-bearing phenocryst phases makes argon-based dating a difficult challenge. As a result, the few absolute eruption age constraints for the pre-caldera deposits of Nisyros, ranging from 0.024 Ma to 0.20±0.05 Ma, are internally discordant (cf. Pe-Piper and Piper, 2002). The Kos Plateau Tuff, which is not found on Nisyros but on surrounding islands, provides a maximum age limit of 161.3±1.1 ka (Smith et al., 1996) for subaerial volcanism on Nisyros. Further, there are no absolute eruption age constraints on the post-caldera domes. However, pumice fall deposits on the nearby island of Yali cover soils that contain neolithic artifacts (Keller, 1982), and while Yali pumice has been found remobilized on talus deposits inside the caldera walls of Nisyros (Volentik et al., 2002), they do not occur on post-caldera dome surfaces or interlayered within dome-related detritus. This suggests that the domes are younger than 10 kyrs.

A number of previous petrological and geochemical studies have provided insights into a variety of petrogenetic processes operating at Nisyros. For the pre-caldera deposits, they include fractional crystallization (Di Paola, 1974), and fractional crystallization combined with assimilation (AFC) of crustal lithologies (Wyers and Barton, 1989). There is also some evidence for magma mixing (Seymour and Vlassopoulos, 1992). Post-caldera rocks show clear evidence of magma mixing as identified through petrographic observations

and trace element geochemistry (Wyers and Barton, 1989; Seymour and Vlassopoulos, 1992). Francalanci et al. (1995) attempted to integrate these processes into a model of magmatic evolution occurring in a single magma reservoir that was active throughout the volcanic history of Nisyros. However, geobarometric data points to a more complicated magma plumbing system in which the dacites and rhyolite magmas crystallized at a deeper level than the mafic magmas (Wyers and Barton, 1989), and recent Sr–Nd–Hf–Pb isotope data document the existence of more than one crustal assimilant during

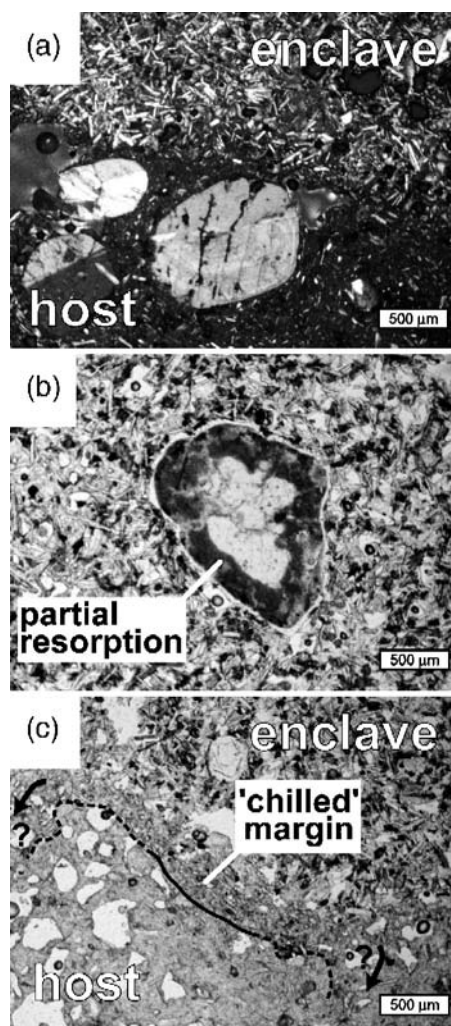


Fig. 3. Photomicrographs of post-caldera dacites and their mafic enclaves. (a) Crossed-polarized light image of rounded plagioclase phenocrysts in the host dacite close to the mafic enclave. (b) Partially resorbed plagioclase crystal within the mafic enclave. (c) Contact between host and the enclave, which in some areas displays a discontinuous fine-crystalline margin. The arrows indicate potential sites of transfer of mafic material into the dacite.

Table 1
Nisyros XRF data

| GZNIS # | 01 | 02 | 03 | 04 | 05x | 06 | 07 | 08 | 09 | 10 | 11 | 12x | 13 | 14 | 15 | 16 | 17 | 18 | 19 |
|--------------------------------|---------|-----------------|-----------------|-----------------|-----------------|-------|-----------------|-------|-------|-----------------|-----------------|-----------------|-----------------|-----------------|-------|-------|-------|-------|-------|
| Unit | ho | lf ⁴ | lf ⁵ | lf ⁵ | lf ⁵ | xlfb | lf ⁶ | alf | alf | lf ⁷ | lf ⁷ | lf ⁷ | lf ⁸ | lf ⁸ | blf | blf | blf | blf | emb |
| Synthem | Kanafia | 2nd Lake | Afonas | Xolante | | | | | | | | | | | | | | | |
| | | | | Fournia | | | | | | | | | | | | | | | |
| SiO ₂ | 54.51 | 59.92 | 58.85 | 57.99 | 57.78 | 66.99 | 58.73 | 71.12 | 71.12 | 64.80 | 64.60 | 46.86 | 58.54 | 54.94 | 55.73 | 59.60 | 59.57 | 55.45 | 66.81 |
| TiO ₂ | 0.93 | 1.12 | 1.11 | 1.07 | 1.06 | 0.65 | 1.11 | 0.36 | 0.36 | 0.50 | 0.50 | 0.68 | 1.08 | 0.92 | 0.82 | 1.13 | 1.13 | 0.95 | 0.62 |
| Al ₂ O ₃ | 17.92 | 16.89 | 17.35 | 17.21 | 17.55 | 15.46 | 17.41 | 14.61 | 14.64 | 16.76 | 16.80 | 15.20 | 17.36 | 18.50 | 18.07 | 16.92 | 16.89 | 18.15 | 15.85 |
| Fe ₂ O ₃ | 7.47 | 7.13 | 7.12 | 7.42 | 7.05 | 4.22 | 7.16 | 2.60 | 2.60 | 4.75 | 4.75 | 6.63 | 7.07 | 7.11 | 5.76 | 7.28 | 7.26 | 7.24 | 4.18 |
| MnO | 0.13 | 0.13 | 0.12 | 0.13 | 0.13 | 0.09 | 0.12 | 0.06 | 0.07 | 0.12 | 0.12 | 0.12 | 0.13 | 0.12 | 0.11 | 0.13 | 0.13 | 0.12 | 0.09 |
| MgO | 4.43 | 2.53 | 2.71 | 3.39 | 2.97 | 1.53 | 2.73 | 0.95 | 0.94 | 1.40 | 1.42 | 7.50 | 2.94 | 4.59 | 4.90 | 2.52 | 2.60 | 4.11 | 1.24 |
| CaO | 9.58 | 5.63 | 6.52 | 6.88 | 6.97 | 3.71 | 6.55 | 2.54 | 2.49 | 4.16 | 4.09 | 22.64 | 6.70 | 8.90 | 9.87 | 5.76 | 5.73 | 8.63 | 3.37 |
| Na ₂ O | 3.61 | 4.32 | 4.15 | 4.03 | 4.57 | 4.31 | 4.10 | 4.27 | 4.18 | 4.92 | 5.06 | 0.27 | 4.19 | 3.56 | 3.37 | 4.32 | 4.26 | 3.90 | 4.49 |
| K ₂ O | 1.23 | 2.09 | 1.82 | 1.65 | 1.70 | 2.88 | 1.82 | 3.37 | 3.40 | 2.40 | 2.47 | 0.01 | 1.74 | 1.14 | 1.15 | 2.08 | 2.16 | 1.20 | 3.17 |
| P ₂ O ₅ | 0.18 | 0.26 | 0.25 | 0.25 | 0.23 | 0.16 | 0.25 | 0.10 | 0.10 | 0.19 | 0.19 | 0.09 | 0.25 | 0.21 | 0.21 | 0.26 | 0.26 | 0.25 | 0.18 |
| (LOI) | 1.30 | -0.01 | -0.02 | -0.19 | -0.27 | 0.73 | -0.01 | 0.01 | -0.53 | 0.89 | 1.47 | 0.12 | 0.12 | -0.20 | 0.80 | -0.27 | 0.84 | -0.08 | 0.92 |
| Rb | 28.3 | 59.2 | 48.9 | 43.2 | 48.8 | 82.5 | 48.7 | 95.2 | 96.4 | 77.8 | 76.1 | 0.5 | 47.5 | 28.3 | 25.3 | 58.1 | 58.0 | 28.4 | 88.1 |
| Sr | 515 | 389 | 378 | 397 | 389 | 286 | 377 | 267 | 263 | 380 | 377 | 271 | 382 | 480 | 595 | 395 | 388 | 515 | 302 |
| Y | 22.7 | 30.4 | 30.9 | 29.2 | 28.0 | 19.9 | 31.1 | 15.0 | 16.0 | 23.2 | 23.6 | 16.4 | 28.7 | 24.8 | 20.4 | 30.2 | 29.4 | 22.7 | 23.7 |
| Zr | 132 | 194 | 182 | 175 | 176 | 168 | 182 | 165 | 166 | 217 | 214 | 89 | 179 | 141 | 125 | 196 | 192 | 144 | 240 |
| Nb | 11.0 | 15.4 | 14.1 | 13.6 | 13.4 | 15.1 | 14.2 | 15.7 | 16.4 | 14.3 | 14.2 | 3.9 | 13.4 | 10.5 | 11.7 | 15.6 | 15.5 | 9.9 | 17.5 |
| Ba | 250 | 509 | 468 | 421 | 418 | 692 | 473 | 819 | 804 | 617 | 609 | 27 | 433 | 311 | 354 | 524 | 512 | 369 | 716 |
| Pb | 5 | 6 | 9 | 9 | 8 | 9 | 9 | 12 | 13 | 15 | 13 | 0 | 8 | 6 | 7 | 11 | 9 | 5 | 12 |
| Th | 4 | 7 | 6 | 7 | 7 | 12 | 6 | 16 | 15 | 9 | 8 | 2 | 6 | 4 | 7 | 7 | 8 | 4 | 9 |
| U | 3 | 2 | 1 | 3 | 3 | 3 | 2 | 5 | 4 | 4 | 2 | 3 | 1 | 2 | 1 | 1 | 1 | 5 | 5 |
| Sc | 20 | 17 | 17 | 23 | 23 | 6 | 22 | 3 | 3 | 5 | 5 | 22 | 22 | 21 | 25 | 19 | 18 | 22 | 7 |
| V | 192 | 209 | 216 | 213 | 216 | 90 | 222 | 37 | 33 | 43 | 39 | 130 | 213 | 187 | 189 | 202 | 195 | 171 | 52 |
| Cr | 24 | 10 | 11 | 11 | 16 | 14 | 9 | 10 | 13 | 6 | 14 | 54 | 14 | 46 | 86 | 14 | 9 | 49 | 8 |
| Co | 34 | 16 | 17 | 20 | 18 | 10 | 17 | 4 | 5 | 6 | 7 | 19 | 17 | 23 | 21 | 16 | 16 | 19 | 5 |
| Ni | 30 | 6 | 10 | 9 | 7 | 6 | 8 | 5 | 5 | 2 | 1 | 26 | 7 | 31 | 29 | 5 | 3 | 28 | 4 |
| Cu | 18 | 23 | 52 | 43 | 43 | 15 | 51 | 6 | 6 | 6 | 6 | 5 | 39 | 33 | 23 | 24 | 26 | 42 | 9 |
| Zn | 69 | 76 | 73 | 68 | 73 | 45 | 73 | 29 | 32 | 64 | 65 | 65 | 73 | 68 | 59 | 71 | 75 | 59 | 46 |
| Ga | 17 | 18 | 19 | 18 | 19 | 15 | 19 | 15 | 14 | 17 | 17 | 13 | 18 | 17 | 16 | 18 | 18 | 18 | 16 |
| Mo | 0 | 1 | 1 | 1 | 1 | 2 | 1 | 2 | 2 | 2 | 1 | 0 | 1 | 0 | 1 | 2 | 1 | 0 | 4 |
| As | 4 | 5 | 5 | 2 | 2 | 3 | 2 | 2 | 7 | 4 | 2 | 0 | 5 | 4 | 0 | 1 | 3 | 1 | 5 |
| S | 77 | 26 | 27 | 31 | 25 | 30 | 23 | 35 | 21 | 158 | 200 | 57 | 378 | 148 | 661 | 24 | 28 | 31 | 26 |

GZNIS sample numbers are those given on Fig. 2. 'x' denotes a xenolith or enclave. Stratigraphic units are those of Volentik et al. (2005a). Major element data are normalized to 100%, LOI values are for information only.

| GZNI# | 20 | 21 | 22x | 23 | 24x | 25x | 26x | 27 | 28 | 29 | 30 | 31x | 32 | 33 | 34x | 35 | 36 | 37x | 38 | 39x |
|--------------------------------|-----------------|-----------------|-------|-------|-------|-------|-------|-------|-------|-------|----------------|-------|-------|-------|-------|-------|-------|-------|-------|-------|
| Unit | vu _i | vu _j | lp | nlf | up | up | pfi |
| Synthem | Loutra | | | | | | | | | | Profitis Ilias | | | | | | | | | |
| | Pali | | | | | | | | | | | | | | | | | | | |
| SiO ₂ | 66.78 | 66.73 | 58.71 | 70.83 | 70.16 | 59.62 | 55.54 | 70.62 | 71.66 | 71.86 | 72.04 | 58.69 | 66.28 | 70.34 | 55.63 | 70.63 | 67.03 | 54.19 | 68.29 | 54.75 |
| TiO ₂ | 0.63 | 0.63 | 1.11 | 0.35 | 0.34 | 0.68 | 0.88 | 0.35 | 0.34 | 0.33 | 0.33 | 1.11 | 0.43 | 0.37 | 0.72 | 0.37 | 0.41 | 0.74 | 0.41 | 0.75 |
| Al ₂ O ₃ | 15.90 | 15.86 | 17.36 | 14.90 | 15.65 | 17.18 | 18.51 | 15.04 | 14.68 | 14.62 | 14.38 | 17.32 | 16.54 | 14.98 | 19.38 | 14.75 | 16.23 | 19.71 | 15.71 | 18.83 |
| Fe ₂ O ₃ | 4.15 | 4.23 | 7.14 | 2.62 | 1.24 | 2.98 | 7.73 | 2.74 | 2.57 | 2.48 | 2.48 | 7.11 | 3.44 | 2.73 | 5.88 | 2.79 | 3.23 | 6.09 | 3.10 | 5.98 |
| MnO | 0.09 | 0.09 | 0.13 | 0.06 | 0.02 | 0.05 | 0.13 | 0.07 | 0.07 | 0.07 | 0.07 | 0.13 | 0.07 | 0.06 | 0.10 | 0.06 | 0.07 | 0.09 | 0.07 | 0.10 |
| MgO | 1.24 | 1.26 | 2.78 | 0.80 | 0.94 | 3.07 | 3.98 | 0.80 | 0.64 | 0.57 | 0.57 | 2.82 | 1.87 | 1.09 | 4.67 | 1.12 | 1.75 | 5.06 | 1.48 | 4.45 |
| CaO | 3.43 | 3.48 | 6.56 | 2.61 | 5.70 | 10.36 | 7.70 | 2.50 | 2.07 | 1.98 | 1.90 | 6.54 | 4.62 | 3.02 | 9.01 | 2.92 | 4.39 | 9.77 | 3.87 | 8.96 |
| Na ₂ O | 4.48 | 4.50 | 4.17 | 4.43 | 5.51 | 5.55 | 3.73 | 4.61 | 4.58 | 4.64 | 4.54 | 4.23 | 4.20 | 4.19 | 3.35 | 4.11 | 4.22 | 3.29 | 4.24 | 4.92 |
| K ₂ O | 3.13 | 3.05 | 1.79 | 3.31 | 0.33 | 3.35 | 1.57 | 3.18 | 3.32 | 3.36 | 3.60 | 1.80 | 2.45 | 3.11 | 1.09 | 3.14 | 2.57 | 0.89 | 2.73 | 1.08 |
| P ₂ O ₅ | 0.17 | 0.18 | 0.25 | 0.08 | 0.10 | 0.16 | 0.22 | 0.08 | 0.06 | 0.08 | 0.08 | 0.25 | 0.11 | 0.09 | 0.17 | 0.10 | 0.10 | 0.17 | 0.11 | 0.19 |
| (LOI) | 1.25 | -0.04 | -0.20 | 2.34 | 0.15 | 0.12 | 0.82 | 1.85 | 1.51 | 0.88 | 3.26 | -0.20 | 0.32 | 0.73 | 0.43 | 0.28 | 0.46 | 0.37 | 0.51 | 0.65 |
| Rb | 88.0 | 88.2 | 52.5 | 96.3 | 2.0 | 2.0 | 32.2 | 91.8 | 96.4 | 101.2 | 96.0 | 52.4 | 70.8 | 95.4 | 20.7 | 95.7 | 76.3 | 12.9 | 82.5 | 14.6 |
| Sr | 308 | 311 | 380 | 258 | 446 | 497 | 674 | 257 | 225 | 213 | 199 | 377 | 491 | 319 | 913 | 309 | 457 | 984 | 417 | 966 |
| Y | 24.1 | 25.6 | 30.3 | 16.9 | 12.9 | 21.6 | 21.2 | 16.9 | 18.7 | 17.9 | 18.8 | 29.5 | 13.8 | 15.5 | 16.9 | 15.5 | 14.7 | 16.8 | 15.3 | 18.7 |
| Zr | 235 | 243 | 187 | 206 | 195 | 118 | 130 | 222 | 235 | 240 | 249 | 187 | 160 | 186 | 113 | 189 | 163 | 108 | 164 | 119 |
| Nb | 17.8 | 18.3 | 13.9 | 15.0 | 8.1 | 12.6 | 9.6 | 15.3 | 15.7 | 17.1 | 16.6 | 14.5 | 11.9 | 14.2 | 7.3 | 14.0 | 11.4 | 6.8 | 12.7 | 7.8 |
| Ba | 714 | 757 | 437 | 741 | 217 | 193 | 434 | 751 | 808 | 768 | 754 | 431 | 597 | 709 | 305 | 727 | 626 | 245 | 632 | 269 |
| Pb | 12 | 8 | 9 | 15 | 4 | 0 | 6 | 15 | 15 | 15 | 15 | 9 | 13 | 12 | 13 | 13 | 11 | 3 | 10 | 6 |
| Th | 12 | 12 | 7 | 13 | 7 | 2 | 4 | 10 | 12 | 12 | 12 | 5 | 9 | 11 | 3 | 11 | 10 | 3 | 11 | 2 |
| U | 5 | 4 | 4 | 4 | 2 | 1 | 2 | 4 | 3 | 4 | 5 | 2 | 3 | 3 | 2 | 4 | 4 | 4 | 4 | 2 |
| Sc | 7 | 6 | 19 | 4 | 1 | 12 | 17 | 1 | 2 | 2 | 3 | 20 | 6 | 3 | 14 | 4 | 5 | 18 | 6 | 11 |
| V | 49 | 58 | 212 | 23 | 33 | 87 | 163 | 25 | 20 | 21 | 16 | 211 | 57 | 32 | 124 | 40 | 53 | 148 | 48 | 140 |
| Cr | 8 | 9 | 12 | 5 | 7 | 20 | 6 | 5 | 11 | 7 | 4 | 17 | 12 | 5 | 16 | 8 | 9 | 16 | 8 | 13 |
| Co | 6 | 7 | 17 | 4 | 2 | 7 | 24 | 3 | 3 | 3 | 3 | 17 | 10 | 6 | 21 | 6 | 7 | 24 | 6 | 21 |
| Ni | 4 | 4 | 7 | 2 | 3 | 8 | 8 | 3 | 4 | 4 | 3 | 8 | 9 | 6 | 26 | 5 | 8 | 28 | 7 | 19 |
| Cu | 8 | 9 | 44 | 5 | 8 | 6 | 19 | 5 | 5 | 4 | 6 | 48 | 14 | 11 | 17 | 7 | 12 | 21 | 12 | 21 |
| Zn | 46 | 42 | 74 | 38 | 11 | 14 | 55 | 39 | 39 | 41 | 43 | 75 | 39 | 32 | 60 | 33 | 37 | 45 | 37 | 51 |
| Ga | 16 | 17 | 18 | 13 | 16 | 17 | 17 | 15 | 14 | 14 | 14 | 18 | 16 | 14 | 18 | 14 | 13 | 18 | 14 | 18 |
| Mo | 4 | 3 | 0 | 4 | 0 | 0 | 0 | 3 | 2 | 3 | 3 | 1 | 2 | 3 | 0 | 1 | 1 | 0 | 2 | 0 |
| As | 8 | 4 | 2 | 4 | 4 | 2 | 0 | 6 | 5 | 5 | 10 | 5 | 6 | 4 | 2 | 7 | 7 | 2 | 8 | 0 |
| S | 31 | 23 | 28 | 29 | 30 | 39 | 95 | 22 | 36 | 22 | 114 | 31 | 28 | 24 | 45 | 55 | 27 | 46 | 36 | 311 |

the magmatic evolution of the volcano (Buettner et al., 2005). The relative importance of the suggested variety of petrogenetic processes will be reassessed in this study.

3. Analytical techniques

All data were collected at the Open University, U.K., at approximately the same time as published data from Santorini (Zellmer et al., 2000). Major and trace elements were analyzed by XRF, and Cs, Zn, Co, Ta, Hf and the rare earth elements by INAA, following standard techniques (Potts et al., 1985; Ramsey et al., 1995). Sr and Nd isotope ratios were determined statically in multi-collector mode on Finnigan MAT 261 and 262 thermal ionization mass spectrometers, over a period of several weeks. Sr was fractionation corrected to $^{86}\text{Sr}/^{88}\text{Sr}=0.1194$, and Nd to $^{146}\text{Nd}/^{144}\text{Nd}=0.7219$. The NBS 987 Sr and the Open University internal Johnson and Matthey (J and M) Nd standards gave running means of $^{87}\text{Sr}/^{86}\text{Sr}=0.71022\pm 0.00003$ (2σ) and $^{143}\text{Nd}/^{144}\text{Nd}=0.511683\pm 0.000030$ (2σ), respectively. To facilitate comparison with data from Santorini published by Zellmer et al. (2000), all samples were normalized to an Open University J and M $^{143}\text{Nd}/^{144}\text{Nd}$ ratio of 0.511836, which corresponds to a La Jolla $^{143}\text{Nd}/^{144}\text{Nd}$ ratio of 0.511865 (Ian Parkinson, pers. comm., 2006). The standard ratios reported here thus correspond closely to the generally accepted ratios of ~ 0.71024 and ~ 0.511860 for the NBS 987 Sr and La Jolla Nd standards, respectively. Blanks were typically <2 ng for Sr, and <500 pg for Nd.

Th and U concentrations and $^{230}\text{Th}/^{232}\text{Th}$ isotope ratios were determined by thermal ionization mass spectrometry on a high abundance sensitivity Finnigan MAT 262, equipped with an RPQ-II energy filter. Samples were spiked with a mixed ^{229}Th – ^{236}U tracer and the dissolution and chemical separation procedures employed were the same as those described by Turner et al. (1996). Mass spectrometric procedures followed those described in van Calsteren and Schwieters (1995), with an external reproducibility of $<1.2\%$ (2σ), monitored using the Th'U' standard. Total procedural blanks for U and Th were typically 100 pg, which is negligible compared to the ~ 500 ng of sample typically loaded. The error on U/Th ratios is $<1.5\%$ (2σ). Decay constants used in the calculation of activity ratios were $\lambda^{230}\text{Th}=9.195\times 10^{-6}$, $\lambda^{232}\text{Th}=4.948\times 10^{-11}$ and $\lambda^{238}\text{U}=1.551\times 10^{-10}$ (Goldstein et al., 1989). Multiple determinations of the ATHO rock standard yielded ($^{230}\text{Th}/^{232}\text{Th}$)= 1.026 ± 0.014 ($n=11$).

4. Results

4.1. Field and petrographic observations

A variety of inclusions are found in deposits from Nisyros. There are holocrystalline xenoliths (e.g. samples GZNis 12x, 24x, and 25x), andesitic lithics (e.g. samples GZNis 05x, 22x and 31x), and most notably mafic enclaves (e.g. samples GZNis 26x, 34x, 37x and 39x) hosted in more evolved rocks. Although mafic enclaves are occasionally found in evolved pre-caldera deposits, they are most abundant in the post-caldera dacites, where they are typically a few cm in size, and have crenulate margins.

Photomicrographs of post-caldera dacites and their mafic enclaves are given in Fig. 3. Host dacites have phenocrysts of plagioclase, amphibole and magnetite set in a fine-grained groundmass of feldspar, amphibole and magnetite. Plagioclase phenocrysts are frequently rounded, especially near contacts with the mafic enclaves (Fig. 3a). The enclaves are phenocryst poor. Their groundmass is coarser grained than that of the host dacite, and diktytaxitic in texture, characterized by randomly oriented elongated microlites of feldspar and amphibole, and some oxides. They also contain some larger crystals of plagioclase that show strong disequilibrium textures such as wide sieve-textured zones of partial resorption (Fig. 3b). In the narrow contact zone to their host rock, the groundmass of the enclaves is in places a little finer grained, displaying a discontinuous 'chilled' margin (cf. Fig. 3c).

4.2. Major and trace element data

New XRF major and trace element data from the youngest eruptive products of Nisyros are given in Table 1. Most samples are typical arc basaltic andesites to rhyolites of calc-alkalic (cf. Peacock, 1931), low- to medium-Fe (cf. Arculus, 2003), and medium- to high-K (cf. Gill, 1981, and Fig. 4a) composition. Although mapping has yielded a complicated ~ 150 ka history of multiple eruptive episodes (Vanderkluyesen et al., 2005; Volentik et al., 2005b), the geochemical trends point to a less complex petrogenetic evolution, and samples from Nisyros have been divided here into pre-caldera and post-caldera host rocks and xenoliths. In pre-caldera samples, FeO, MgO, CaO, Al_2O_3 and Sr are compatible; K_2O , Rb and Ba are incompatible, as are Zr and Nb except in some high silica rocks; and TiO_2 , Na_2O , P_2O_5 and Y are incompatible in low silica and compatible in high silica rocks. Post-caldera samples have slightly lower K_2O , Rb, Y, Zr, Nb and Ba, and slightly higher Sr

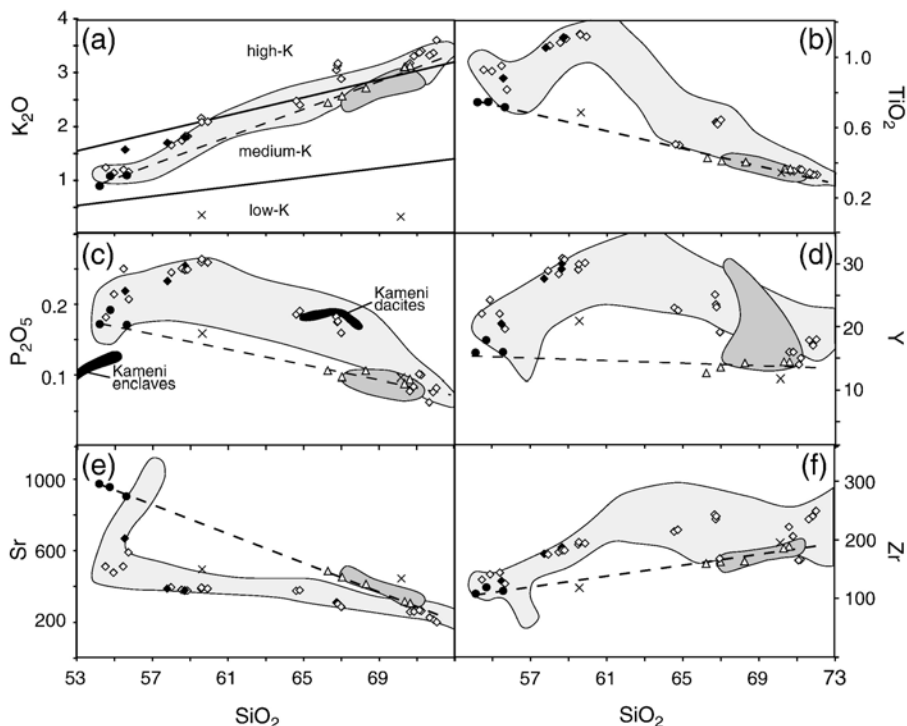


Fig. 4. Major element oxide and trace element variation diagrams of Nisyros samples, with SiO_2 as differentiation index. Symbols: (\diamond) pre-caldera rocks; (\blacklozenge) pre-caldera lithics and enclaves; (\times) holocrystalline xenoliths, sample GZNis 12x omitted for scaling purposes; (\triangle) post-caldera dacites; (\bullet) post-caldera mafic enclaves. Shaded fields represent previously published data of pre-caldera (light grey) and post-caldera (dark grey) rocks (Francalanci et al., 1995; Buettner et al., 2005), while solid fields in (c) represent are data for Santorini's post-caldera Kameni dacites and their enclaves (Zellmer et al., 2000). See text for discussion.

concentrations than pre-caldera samples (cf. Fig. 4). Further, the post-caldera dacites define a straight trend which projects back to their mafic enclaves, particularly obvious in terms of Sr and TiO_2 versus SiO_2 . The high-silica end of this trend has high Sr concentrations and low TiO_2 , P_2O_5 , Y and Zr concentrations compared to most pre-caldera samples (cf. Fig. 4).

Rare earth element (REE) and trace element INAA data of selected samples are given in Table 2, and chondrite-normalized REE abundance patterns are potted in Fig. 5. The light rare earth elements (LREE), La to Nd, are enriched relative to the middle rare earths (MREE), Pm to Ho, and heavy rare earths (HREE), Er to Lu. The LREE enrichment is more pronounced in the post-caldera dacites, which also display distinctive trough-shaped patterns in the MREE and HREE. These features point to an involvement of amphibole in the petrogenesis of the post-caldera dacites, either as a crystallizing phase or in the residue during melting (e. g. Tiepolo et al., 2000, and references therein). One mafic enclave has been analyzed and has a REE pattern similar to the pre-caldera samples, but is lacking a weak negative Eu anomaly that is observed in most other samples.

4.3. Isotope data

New Sr–Nd isotope data are given in Table 3 and plotted in Fig. 6. Two compositional groups are apparent: the dacites and the mafic inclusions define a linear trend towards low $^{143}\text{Nd}/^{144}\text{Nd}$ ratios, while three more mafic pre-caldera samples yield higher $^{87}\text{Sr}/^{86}\text{Sr}$ and $^{143}\text{Nd}/^{144}\text{Nd}$ ratios and lie within the trend defined by the Santorini samples (Fig. 6a). Fig. 6b shows increasing $^{87}\text{Sr}/^{86}\text{Sr}$ with increasing SiO_2 for both compositional groups, suggesting that Sr–Nd isotopic changes occur during magmatic differentiation and are therefore likely to be due to assimilation of two isotopically distinct lithologies during crustal magma evolution.

U–Th disequilibria are shown on an equiline diagram in Fig. 7. Most samples are in U–Th equilibrium or have small ^{238}U excesses. At Nisyros, the post-caldera dacites have $(^{238}\text{U}/^{232}\text{Th})$ ratios between 0.84 and 0.87, and $(^{230}\text{Th}/^{232}\text{Th})$ ratios between 0.82 and 0.86. The mafic enclaves display slightly greater $(^{238}\text{U}/^{232}\text{Th})$ ratios between 0.92 and 1.04, and one enclave (GZNis 37x) displays the greatest U-excess (although still only $\sim 10\%$). A reference line through this enclave and the

Table 2
Nisyros INAA data

| GZNis # | 03 | 08 | 10 | 14 | 16 | 21 | 35 | 36 | 37x |
|---------|-----------------|------|-----------------|-----------------|---------|-----------------|----------------|------|------|
| Unit | lf ⁵ | alf | lf ⁷ | lf ⁸ | blf | vu ₁ | pfi | pfi | pfi |
| Synthem | Afionas | | | Xolante | Fournia | Loutra | Profitis Ilias | | |
| La | 27.2 | 36.0 | 31.1 | 18.8 | 20.0 | 35.3 | 30.2 | 27.1 | 14.0 |
| Ce | 50.6 | 59.4 | 56.8 | 38.2 | 40.6 | 62.1 | 52.2 | 46.7 | 28.6 |
| Nd | 23.8 | 18.3 | 21.7 | 18.6 | 18.8 | 23.7 | 17.0 | 16.1 | 15.1 |
| Sm | 4.97 | 3.29 | 4.15 | 3.97 | 3.81 | 4.57 | 3.14 | 3.00 | 3.37 |
| Eu | 1.32 | 0.67 | 1.05 | 1.17 | 1.12 | 1.02 | 0.61 | 0.75 | 1.10 |
| Tb | 0.81 | 0.39 | 0.60 | 0.66 | 0.62 | 0.68 | 0.40 | 0.39 | 0.52 |
| Yb | 3.10 | 1.81 | 2.72 | 2.40 | 2.35 | 2.71 | 1.85 | 1.67 | 1.60 |
| Lu | 0.46 | 0.29 | 0.42 | 0.37 | 0.35 | 0.42 | 0.29 | 0.27 | 0.24 |
| Th | 5.9 | 13.4 | 8.5 | 3.6 | 3.5 | 11.4 | 12.0 | 9.3 | 1.8 |
| U | 2.0 | 3.9 | 2.6 | 1.1 | 1.4 | 3.7 | 3.3 | 2.6 | n/d |
| Ta | 0.90 | 1.31 | 1.04 | 0.66 | 0.56 | 1.30 | 1.19 | 0.93 | 0.33 |
| Hf | 4.32 | 4.00 | 4.84 | 3.26 | 3.29 | 5.47 | 4.64 | 3.81 | 2.72 |
| Cs | 1.22 | 1.59 | 3.05 | 1.00 | 0.80 | 1.65 | 2.37 | 2.71 | 0.30 |
| Rb | 51 | 98 | 80 | 43 | 37 | 83 | 92 | 73 | 17 |
| Zn | 103 | 30 | 62 | 67 | 58 | 44 | 34 | 38 | 72 |
| Co | 14.9 | 4.2 | 6.0 | 20.6 | 17.5 | 6.3 | 5.0 | 7.6 | 20.6 |
| Cr | 11 | 10 | 5 | 41 | 47 | 6 | 6 | 6 | 19 |
| Sc | 20.7 | 4.6 | 5.2 | 21.0 | 20.1 | 7.9 | 4.8 | 6.8 | 17.2 |

GZNis sample numbers are those given on Fig. 2. 'x' denotes a xenolith or enclave. Stratigraphic units are those of Volentik et al. (2005a).

highest ($^{238}\text{U}/^{230}\text{Th}$) dacite yields an age of ~ 104 ka, which compares to a post-caldera whole-rock isochron age of ~ 140 ka for Santorini.

5. Discussion

5.1. Magmatic evolution at Nisyros

The major and trace element trends of many pre-caldera products from Nisyros are very similar to those displayed by samples from Santorini (cf., Huijsmans et al., 1988; Zellmer et al., 2000), pointing to comparable petrogenetic processes at depth, dominated by fractional crystallization. From Fig. 4 it is apparent that the fractionating mineral assemblage includes titanomagnetite (TiO_2 begins to decrease at ~ 59 wt% SiO_2), apatite (P_2O_5 and Y begin to decrease at ~ 60 wt.% SiO_2), and zircon in the high silica samples (evidenced by Zr leveling out at ~ 250 ppm and decreasing to < 200 ppm in some samples). There is also petrographic evidence for the crystallization of all of these phases at Nisyros, and their participation in magmatic differentiation through crystal fractionation has been modeled previously (Wyers and Barton, 1989). Thus, while magma mixing may occur across small compositional ranges, the data preclude extensive mixing between mafic and felsic magmas for the pre-caldera samples (cf. Zellmer et al., 2005).

The post-caldera dacites of Nisyros are depleted in MREE and HREE and have a steeper LREE trend compared to the pre-caldera rocks, indicating that amphibole was a prominent phase in their differentiation history. Further, the post-caldera dacites of Nisyros fall off the pre-caldera trends for a number of elements, forming mixing lines towards the mafic enclaves. The crenulated and in places chilled margins (cf. Fig. 3c) of the mafic enclaves, and their diktytaxitic textures, indicate that they are of magmatic origin and were quenched during mingling and partial mixing with the cooler host dacite prior to eruption. The large, partially resorbed plagioclase crystals within the mafic enclaves (cf. Fig. 3b) are interpreted to represent phenocrysts that have originally grown within the host dacite and have subsequently been taken up into the enclave. Further, Wyers and Barton (1989) found petrographic evidence for liberation of amphibole crystals from the mafic inclusions, and mixing of the hot mafic material into the cooler dacitic host is also consistent with the discontinuity of the enclaves' margins (cf. Fig. 3c). Thus, a compositional range is introduced into the post-caldera dacites by mixing up to $\sim 30\%$ towards the enclaves due to incorporation of mafic enclave material into the dacites, while enclave compositions vary by a significantly smaller amount due to limited incorporation of crystals from the dacites into the mafic enclaves.

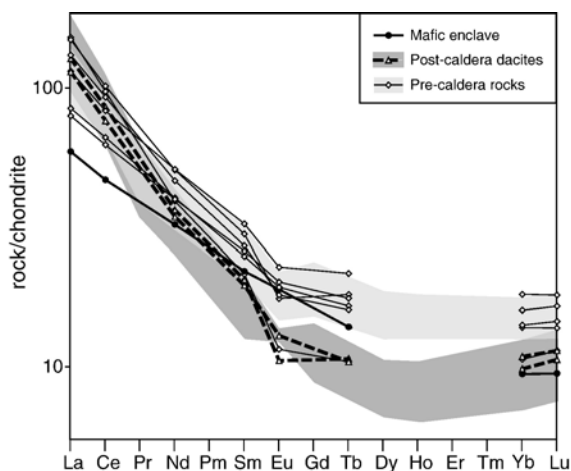


Fig. 5. Chondrite-normalised rare earth element (REE) patterns of Nisyros samples. Normalising values are taken from Sun and McDonough (1989). Pr, Pm and Gd are interpolated between the adjacent REEs. Data from Buettner et al. (2005) are shown as shaded fields for comparison, and provide additional constraints on the middle REEs. See text for discussion.

The Sr–Nd isotope data indicates that some crustal assimilation also occurred during the petrogenesis of the Nisyros rocks. However, it appears that more than one assimilant is present beneath Nisyros, consistent with recent results of Buettner et al. (2005). One of the assimilants to the less evolved pre-caldera samples may be old crust similar to that proposed for Santorini (Zellmer et al., 2000), although the amount of assimilation small (less than $\sim 10\%$, cf. Fig. 6a). In contrast, the more evolved samples, including all of the post-caldera rocks, define a mixing trend with a high silica composition that is significantly younger than upper continental crust (cf. Figs. 4 and 6b), and is therefore likely to be of magmatic origin.

In summary, the data suggests that at Nisyros, two modes of magmatic evolution have been operating: For most pre-caldera rocks, fractional crystallization and assimilation of small amounts of various crustal materials, including old crust, dominated magmatic differentiation. Although the existence of some mafic enclaves within the pre-caldera samples suggests that magma mixing may also have been operating, the inflexions in the major and trace element trends (Fig. 4) indicate that hybridization was not extensive, and that mixing affected the bulk geochemistry of the magmas only to a limited degree. In contrast, the petrogenesis of the post-caldera dacites involved exclusively magmatic components, and there is no evidence for contributions from old crustal sources. While their original magmatic differentiation was affected by amphibole as a major

fractionating phase, their final compositional range largely resulted from mixing with mafic magmas represented by the enclaves. Remobilization of porphyritic silicic host magmas through influx of mafic melts that provide heat and volatiles has also been invoked at other arc volcanoes and may be a widely applicable process in the petrogenesis of intermediate arc magmas (e.g., Murphy et al., 2000; Pichavant et al., 2002; Mortazavi and Sparks, 2004; Zellmer and Clavero, 2006).

5.2. Insights from U-series isotope data from Nisyros and Santorini

As the pre-caldera samples from Nisyros and Santorini straddle the U–Th equiline (Fig. 7), the U–Th system is not suitable for providing much insight into the timing of their petrogenesis. Hence, this study focuses on the post-caldera dacites and their mafic enclaves. All but one of the studied mafic enclaves have U excesses and U/Th ratios significantly greater than those of their host lavas (Fig. 7). Therefore, any simple petrogenetic models that relate mafic and felsic magmas by fractional crystallization through time (cf. Fig. 1a) or by mixing with old evolved lavas derived by fractional crystallization from mafic melts (cf. Fig. 1b) are not plausible, and more complicated scenarios need to be considered to explain a potential genetic relationship between the felsic hosts and their mafic enclaves. If the observed range in ($^{238}\text{U}/^{230}\text{Th}$) ratios was introduced during magmatic differentiation within the arc crust, mixing of mafic melts with more evolved compositions that have lower ($^{238}\text{U}/^{230}\text{Th}$) ratios may in principle be a viable mechanism for the genesis of intermediate arc magmas (cf. Fig. 1c). However, old continental crust has high $^{87}\text{Sr}/^{86}\text{Sr}$ and low $^{143}\text{Nd}/^{144}\text{Nd}$ isotope ratios, and because the U–Th and Sr–Nd isotopic data presented here cannot be reconciled through assimilation with such a component, old continental crust is not a suitable assimilant in the petrogenesis of the post-caldera dacites. In the case of Nisyros, a younger assimilant is required.

One possible model of dacite petrogenesis consistent with the data from Nisyros is given in Fig. 8. Here, new primary arc magmas have ^{238}U excesses (that may or may not be constant through time). Due to the crustal density barrier, these melts stall and age towards U–Th equilibrium when they reach the lower crustal hot zone (cf. Annen and Sparks, 2002; Zellmer et al., 2005). Within the hot zone, thermal equilibration of the basalts will result in the production of small fractions of hydrous felsic residual melts through incomplete basalt

Table 3
Nisyros TIMS data

| GZNIIS # | 01 | 03 | 08 | 12x | 18 | 21 | 33 | 34x | 36 | 37x | 38 | 39x |
|---|----------|-----------------|----------|-----------------|----------|-----------------|----------------|----------|----------|----------|----------|----------|
| Unit | ho | lf ⁵ | alf | lf ⁷ | b1f | vu ₁ | pfi | pfi | pfi | pfi | pfi | pfi |
| Synthem | Kanafia | Afionas | | | Foumia | Loutra | Profitis Ilias | | | | | |
| ⁸⁷ Sr/ ⁸⁶ Sr | 0.704290 | 0.704547 | 0.704146 | | 0.704261 | 0.704021 | 0.704158 | 0.703828 | 0.704040 | 0.703811 | 0.704055 | 0.703795 |
| ±1σ (×10 ⁻⁶) | 9 | 7 | 9 | | 8 | 8 | 8 | 7 | 8 | 10 | 6 | 7 |
| ¹⁴³ Nd/ ¹⁴⁴ Nd | 0.512837 | 0.512830 | | | 0.512807 | 0.512732 | 0.512653 | 0.512764 | 0.512730 | 0.512796 | 0.512702 | |
| ±1σ (×10 ⁻⁶) | 6 | 5 | | | 5 | 8 | 13 | 9 | 5 | 5 | 10 | |
| U (ppm) | 1.093 | 1.636 | 3.623 | 1.729 | 1.025 | | 3.128 | 0.779 | 2.555 | 0.594 | 2.762 | 0.664 |
| ±2σ | 0.003 | 0.003 | 0.005 | 0.004 | 0.003 | | 0.006 | 0.001 | 0.003 | 0.001 | 0.006 | 0.001 |
| Th (ppm) | 3.320 | 5.405 | 12.499 | 2.293 | 3.401 | | 11.097 | 2.573 | 8.883 | 1.740 | 9.998 | 1.950 |
| ±2σ | 0.021 | 0.024 | 0.062 | 0.005 | 0.040 | | 0.155 | 0.015 | 0.061 | 0.015 | 0.135 | 0.012 |
| (²³⁴ U/ ²³⁸ U) | 1.015 | 1.002 | 0.999 | 1.007 | 0.997 | | 1.003 | 1.006 | 1.003 | 1.004 | 0.999 | 1.015 |
| ±2σ | 0.008 | 0.004 | 0.005 | 0.004 | 0.006 | | 0.005 | 0.004 | 0.003 | 0.005 | 0.006 | 0.005 |
| (²³⁸ U/ ²³² Th) | 0.999 | 0.919 | 0.880 | 2.288 | 0.914 | | 0.855 | 0.919 | 0.873 | 1.036 | 0.838 | 1.034 |
| ±2σ | 0.007 | 0.004 | 0.005 | 0.007 | 0.011 | | 0.012 | 0.006 | 0.006 | 0.009 | 0.011 | 0.007 |
| (²³⁰ Th/ ²³² Th) | 1.011 | 0.915 | 0.898 | 2.657 | 0.897 | | 0.825 | 0.894 | 0.861 | 0.937 | 0.824 | 0.987 |
| ±2σ | 0.016 | 0.009 | 0.009 | 0.024 | 0.006 | | 0.009 | 0.005 | 0.008 | 0.009 | 0.010 | 0.007 |

GZNIIS sample numbers are those given on Fig. 2. 'x' denotes a xenolith or enclave. Stratigraphic units are those of Volentik et al. (2005a).

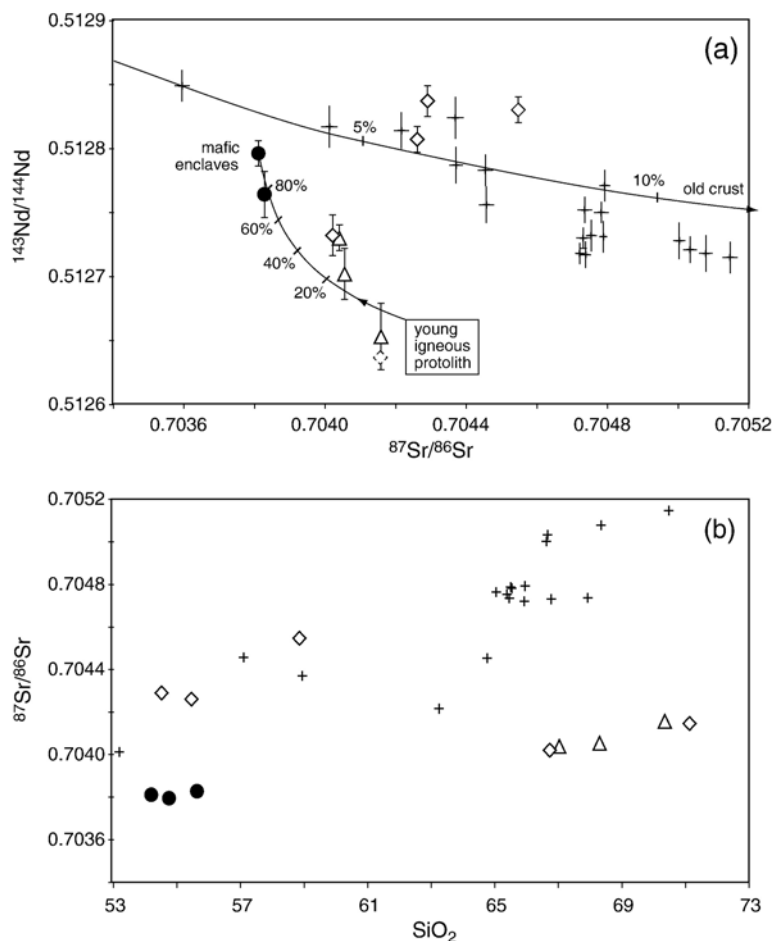


Fig. 6. Variation of (a) $^{143}\text{Nd}/^{144}\text{Nd}$ with $^{87}\text{Sr}/^{86}\text{Sr}$ and (b) $^{87}\text{Sr}/^{86}\text{Sr}$ with SiO_2 , for samples from Nisyros. Symbols: (◇) pre-caldera rocks; (△) post-caldera dacites; (●) post-caldera mafic enclaves. In (a), the $^{143}\text{Nd}/^{144}\text{Nd}$ ratio of the broken diamond is inferred from its $^{87}\text{Sr}/^{86}\text{Sr}$ ratio and the linearity of the low $^{87}\text{Sr}/^{86}\text{Sr}$ trend in (b). Samples from Santorini (+) and the mixing vector towards radiogenic crust are taken from Zellmer et al. (2000) and are given for comparison. Mixing between mafic compositions and a young igneous protolith was approximated by using a mafic enclave and one of the most evolved dacitic hosts as mixing endmembers. See text for discussion.

crystallization. These melts are highly differentiated, and their equilibrium phase assemblage includes amphibole, resulting in trough shaped middle and heavy REE pattern (cf. Fig. 5). Equilibrium phases also include accessory minerals such as zircon, resulting in significant U–Th fractionation. The hydrous silicic melts will be segregated through compaction: a melt fraction of 2% may segregate within 170 kyrs (Jackson et al., 2003), or faster if deformation accelerates this process (Petford et al., 2000). They will ascend to mid or upper crustal levels where they will stall by degassing induced crystallization, forming porphyritic host magmas. These young (in terms of Sr and Nd isotopic composition) protoliths may have significant ^{230}Th excesses, which will decay with time towards U–Th equilibrium at low ($^{238}\text{U}/^{232}\text{Th}$) activity ratios. Finally, influx

of more mafic magma will lead to remobilization of the silicic protolith, yielding dacites like those erupted during the post-caldera phase at Nisyros.

The feasibility of this model with respect to the available U-series data is dependent on the stability of zircon under the above conditions, and the partitioning of U and Th into this phase. The stability of zircon can be evaluated following the approach of Charlier et al. (2005): by comparing the magma temperature (as derived from oxide equilibria) with the zircon saturation temperature, which depends on the Zr content of the melt and its cation ratio $(\text{Na} + \text{K} + 2\text{Ca})/(\text{Al} \times \text{Si})$ (Watson and Harrison, 1983). Magma temperatures of the post-caldera domes range from 804 to 843 °C based on ilmenite-ulvospinel geothermometry (Seymour and Lalonde, 1991), and compare favorably to a zircon

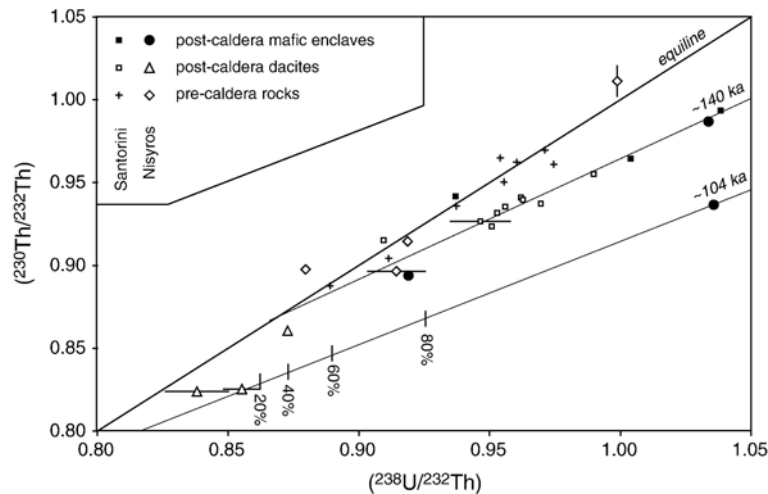


Fig. 7. U–Th equiline diagram summarizing available data from Nisyros (this study) and Santorini (Zellmer et al., 2000) for pre-caldera rocks, and for the post caldera host rocks and their mafic enclaves (see key to symbols). Holocrystalline xenolith GZNis 12x has been omitted for scaling purposes. Analytical errors are less than 1.0% (2σ) on $(^{238}\text{U}/^{232}\text{Th})$ and less than 1.2% (2σ) on $(^{230}\text{Th}/^{232}\text{Th})$ activity ratios, unless indicated otherwise. Due to a lack of eruption age constraints at Nisyros, $(^{230}\text{Th}/^{232}\text{Th})$ activity ratios have not been corrected for radioactive decay since eruption, but post-caldera samples from Nisyros are younger than ~ 10 ka. A post-caldera whole-rock isochron from Santorini, and a post-caldera reference line through host and enclave with the largest ^{238}U excesses from Nisyros, yield ages of ~ 140 ka and ~ 104 ka, respectively. Mixing proportions were added to the 104 ka reference line for comparison with Fig. 6a, and confirms that the observed range in $(^{238}\text{U}/^{230}\text{Th})$ in the mafic enclaves is expected from mixing with their host dacites that have significantly higher U and Th concentrations.

saturation temperature of ~ 813 °C using one of the most evolved post-caldera dacites (GZNis 33) as a composition that closely resembles the modeled igneous protolith. This suggests that zircon may be stable, consistent with the observed occurrence of zircon microphenocrysts within the dacites (Wyers and Barton, 1989). Relative partitioning of U and Th into zircon can be evaluated from the literature, where the $D_{\text{U}}/D_{\text{Th}}$ exchange coefficient between zircon and melt varies between 2.6 and 6.3, and where zircon U and Th concentrations of up to 2360 and 3710 ppm, respectively, have been reported (Pyle et al., 1988), although concentrations of the order of 300 ppm appear to be more common (cf., Condomines, 1997; Charlier and Zellmer, 2000; Heumann et al., 2002; Charlier et al., 2005). Depending on the choice of zircon U and Th concentrations (e.g. 300–3000 ppm), removal of 0.03–0.3% (i.e. trace amounts) of zircon by crystal fractionation will result in the observed range in $(^{238}\text{U}/^{230}\text{Th})$ of ~ 0.2 on Fig. 7, indicating that the petrogenetic model of remobilization of a igneous protolith, as outlined above, is indeed feasible for Nisyros.

In striking contrast, for Santorini volcano magma mixing had very limited influence in the bulk geochemical evolution of the post-caldera dacites: although a variety of mafic enclaves occur within the post-caldera dacites (e.g., Nicholls, 1971; Martin et al., 2006) and are interpreted to represent influxing mafic magmas respon-

sible for triggering volcanic eruption (Holness et al., 2005; Martin et al., 2006), and although some phenocrysts in the host rocks may be derived from complete

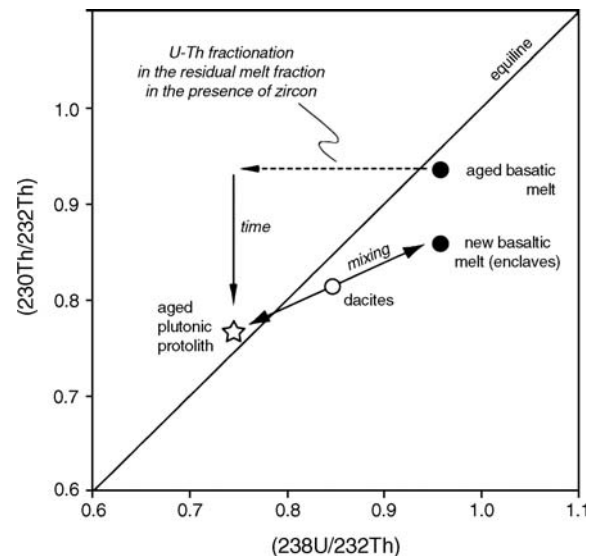


Fig. 8. Petrogenetic model for the post-caldera samples of Nisyros. Highly evolved residual melts, in equilibrium with zircon, segregate from aged basaltic melts to form an arc protolith in ^{230}Th excess. With time, the young protolith will age towards U–Th equilibrium. Influx of new basaltic melt into this system results in remobilization of the protolith by mingling and mixing, and in the extrusion of the post-caldera dacites and their mafic enclaves. See text for discussion.

breakup of the mafic enclaves (Martin et al., 2006), the inflexion of P_2O_5 within the post-caldera dacites (cf. Fig. 4c) precludes that their range in silica content is the result of mixing with mafic magmas represented by the enclaves. In addition, the modest compositional discontinuities in An content (≤ 10 mol%) of plagioclase crystals within the host rocks (Stamatelopoulou-Seymour et al., 1990) suggests that thermal perturbations rather than chemical hybridization dominated their recent evolution. Hence, in Santorini the observed range in ($^{238}U/^{232}Th$) ratios (Fig. 7) may be a source feature. Petrogenetic scenarios that invoke aging during fractional crystallization (cf. Fig. 1a), but limited mixing with older lavas of similar ($^{238}U/^{232}Th$) composition (cf. Fig. 1b), are thus a viable mechanism in the genesis of Santorini's post-caldera dacites if their parental melts were variably enriched in ^{238}U (cf. Zellmer et al., 2000).

Finally, it may be speculated that the two pathways of intermediate magma genesis presented here do not only control the geochemistry of the erupted lavas, but also the style of their eruption. Texturally, the post-caldera dacites of Nisyros have a much higher phenocryst content of 25–40 vol.% (Francalanci et al., 1995) than the post-caldera dacites of Santorini with typically 15 vol.% (Higgins, 1996). The high crystallinity of the Nisyros dacites is consistent with the suggested remobilization of a porphyritic igneous protolith, as opposed to the simpler differentiation mechanisms invoked for Santorini's post-caldera magmas, which may have been prevented from further crystallization due to repeated influx of hot mafic melts that ponded at the base of the dacitic magma reservoir as suggested by Holness et al. (2005). In consequence, the Santorini dacites were erupted as lava flows, while the Nisyros dacites extruded as more viscous porphyritic lava domes, similar to other arc lava eruptions that have been linked to remobilization of igneous protoliths (e.g., Murphy et al., 2000; Zellmer and Clavero, 2006).

5.3. Implications for the rates of magma ascent through the crust

Although the petrogenetic histories of some intermediate arc magmas appear to be complicated, it is nevertheless possible to extract valuable age information using U-series isotopes. At Santorini, most of the post-caldera dacites form a tight isochron with two of the three analyzed mafic enclaves, yielding an age of ~ 140 ka. The third enclave lies off this trend on the equiline, and is therefore probably older and may be petrogenetically unrelated to the other samples (cf.

Zellmer et al., 2000). At Nisyros, there are significant differences between mafic enclaves and host andesites in terms of their rare earth element pattern (Fig. 5), suggesting that in this system, enclaves and hosts are not related through a simple petrogenetic process. It is therefore not possible to obtain a reliable isochron with geological significance. However, given that Santorini and Nisyros are part of the same volcanic arc, it may be reasonable to argue for a similar initial ($^{230}Th/^{232}Th$) isotopic ratio of ~ 0.8 – 0.85 for their source. Hence, an approximate minimum age reference line may be obtained using the Nisyros samples with the lowest ($^{230}Th/^{232}Th$) and highest ($^{238}U/^{230}Th$) activity ratios. Taking this approach yields a minimum age of U-enrichment in the source of ~ 104 ka, within 2σ error of the Santorini whole-rock isochron of ~ 140 ka (Fig. 7). This suggests that in both volcanic systems studied here, more than ~ 100 kyrs may have elapsed between U-enrichment of the source and the eruption of the mafic enclaves within their intermediate host lavas.

U-enrichment timescales of ≥ 100 kyrs obtained from mafic enclaves in intermediate arc volcanoes are on the upper end of those estimated for the eruptive products of mafic arc volcanoes, which frequently display higher ^{238}U excesses of up to 80% (e.g., Turner et al., 2001, 2003; Reagan et al., 2003; Zellmer et al., 2005). Although the total number of mafic enclaves analyzed for U-series isotopes is still low, one may speculate at this point that in intermediate systems, which are generally more mature than mafic arc volcanoes in that they have experienced prolonged periods of intrusive activity, new mafic magmas tend to stall within the crust more frequently due to density contrasts with previous intrusives of more evolved composition, resulting in slower crustal magma transfer times. This points to a link between the U-series chemistry of mafic arc magmas and the mode of their occurrence, with mafic enclaves generally displaying lower ^{238}U excesses than more voluminous mafic eruptive products. Future studies of ^{226}Ra – ^{230}Th disequilibria in mafic enclaves are one avenue to test this hypothesis.

Finally, the data presented here also puts some constraints on the timing of silicic melt generation at arcs. In the case of the post-caldera dacites of Santorini, where magma mixing is of little importance, the dacites form a ~ 140 ka isochron with their mafic enclaves, suggesting that this is the maximum time required to form dacitic melts through differentiation from primary arc basalts. In the case of the post-caldera dacites of Nisyros, where mixing appears to be an important process, none of the lavas have ^{230}Th excesses, implying that the inferred igneous protolith is close to

U–Th equilibrium and therefore had a crustal residence time of at least ~ 350 kyrs. Intrusion of the silicic protolith therefore predates any subaerial volcanism at Nisyros, providing evidence for a prolonged magmatic history in the area.

6. Conclusions

1. Mafic enclaves are found in many intermediate arc magmas. In the post-caldera samples from Nisyros, they are frequently rounded, and some have crenulate and in places chilled margins. They trap phenocrysts that likely crystallized within their host magma, leading to prominent resorption textures. Crystals within the host rock also display disequilibrium textures, probably resulting from an increase in magmatic temperature prior to eruption. These textural features imply influx, mingling and small scale mixing of hot mafic magma into a cooler reservoir of intermediate composition prior to eruption.
2. Most pre-caldera lavas of Nisyros display geochemical trends that suggest a petrogenetic history involving significant fractional crystallization, some crustal assimilation, and rather limited amounts of mixing. In contrast, the post-caldera dacites of Nisyros show ample geochemical evidence for magma mixing towards their mafic enclaves.
3. U–Th isotopes preclude simple models that relate dacites to their mafic enclaves by crystal fractionation or aging alone. The Sr and Nd isotopic composition of Nisyros' post-caldera dacites points to a young magmatic pluton as their source. Remobilization of such a pluton is consistent with the U–Th isotopic composition of the dacites and their mafic enclaves if accessory phases such as zircon can be invoked to be stable during the petrogenesis of the felsic protolith. In contrast, while there is evidence for magma mixing at Santorini, it does not result in significant chemical hybridization in the post-caldera dacites, and there the observed range in U–Th ratios may thus be a source feature.
4. One may speculate that as a rule, intermediate composition porphyritic lava *domes* (e.g. as erupted in Montserrat, Nisyros and Taapaca) commonly represent remobilized plutons. In contrast, in terms of their bulk geochemistry, intermediate composition lava *flows* with lower crystallinity (e.g. Santorini's post-caldera dacites) seem to have less complicated petrogenetic histories and may preserve primary signatures.
5. Despite the different petrogenetic pathways of post-caldera dacites in Santorini and Nisyros, U–Th disequilibria yield time scales of ≥ 100 kyrs for the mafic enclaves in both systems. This suggests that in mature volcanic arcs such as the Aegean arc, mafic enclaves in intermediate host lavas have relatively long crustal residence times compared to some less evolved arc volcanoes, where mafic eruptive products may have crustal residence times of days or less.
6. The available U-series data suggests that differentiation from primary arc basalts to intermediate compositions typically requires less than ~ 140 ka, and that the age of young silicic plutons remobilized by mafic arc magmas is of the order of at least 350 kyrs, in places predating the subaerial history of volcanism in the Aegean arc.

Acknowledgements

We thank Julie Hardiman for her helpful advice regarding fieldwork on Nisyros. Field assistance was fearlessly provided by Rhiannon George. INAA analyses were performed by Nick Rogers. Louise Thomas and John Watson helped with Sr–Nd isotope and XRF analyses, respectively. Loïc Vanderkluyzen correlated sampling locations to the new stratigraphy. We gratefully acknowledge Julia Hammer, Chris Hawkesworth, Steve Sparks and Loïc Vanderkluyzen for thought-provoking discussions. We thank two anonymous reviewers for their constructive comments and Stephen Foley for editorial handling of this manuscript. GFZ acknowledges funding by the Institute of Earth Sciences, Academia Sinica, and also a SOEST post-doctoral stipend and an Open University studentship. SPT acknowledges an ARC Federation fellowship and a Royal Society fellowship.

References

- Annen, C., Sparks, R.S.J., 2002. Effects of repetitive emplacement of basaltic intrusions on thermal evolution and melt generation in the crust. *Earth and Planetary Science Letters* 203, 937–955.
- Arculus, R.J., 2003. Use and abuse of the terms calcalkaline and calcalkalic. *Journal of Petrology* 44, 929–935.
- Bacon, C.R., 1986. Magmatic inclusions in silicic and intermediate volcanic rocks. *Journal of Geophysical Research* 91, 6091–6112.
- Buettner, A., Kleinhanns, I.C., Rufer, D., Hunziker, J.C., Villa, I.M., 2005. Magma generation at the easternmost section of the Hellenic arc: Hf, Nd, Pb and Sr isotope geochemistry of Nisyros and Yali volcanoes (Greece). *Lithos* 83, 29–46.
- Charlier, B.L.A., Zellmer, G.F., 2000. Some remarks on U–Th mineral ages from igneous rocks with prolonged crystallisation histories. *Earth and Planetary Science Letters* 183, 457–469.
- Charlier, B.L.A., Wilson, C.J.N., Lowenstern, J.B., Blake, S., van Calsteren, P.W., Davidson, J.P., 2005. Magma generation at a large,

- hyperactive silicic volcano (Taupo, New Zealand) revealed by U–Th and U–Pb systematics in zircons. *Journal of Petrology* 46, 3–32.
- Clynne, M.A., 1999. A complex magma mixing origin for rocks erupted in 1915, Lassen Peak, California. *Journal of Petrology* 40, 105–132.
- Condomines, M., 1997. Dating recent volcanic rocks through ^{230}Th – ^{238}U disequilibrium in accessory minerals: example of the Puy de Dome (French Massif Central). *Geology* 25 (4), 375–378.
- Condomines, M., Gauthier, P.-J., Sigmarrsson, O., 2003. Timescales of magma chamber processes and dating of young volcanic rocks. In: Bourdon, B., Henderson, G.M., Lundstrom, C.C., Turner, S.P. (Eds.), *Uranium-Series Geochemistry. Reviews in Mineralogy and Geochemistry*. The Mineralogical Society of America, Washington, pp. 125–174.
- Di Paola, G.M., 1974. Volcanology and petrology of Nisyros island (Dodecanese Greece). *Bulletin of Volcanology* 38, 944–987.
- Francalanci, L., Varekamp, J.C., Vougioukalakis, G., Defant, M.J., Innocenti, F., Manetti, P., 1995. Crystal retention, fractionation and crustal assimilation in a convecting magma chamber, Nisyros Volcano, Greece. *Bulletin of Volcanology* 56, 601–620.
- Francis, P.W., Horrocks, L., Oppenheimer, C.M.M., 2000. Monitoring gases from andesite volcanoes. *Philosophical Transactions of the Royal Society of London*. A 358, 1567–1584.
- Gill, J.B., 1981. *Orogenic Andesites and Plate Tectonics*. Springer Verlag, Heidelberg.
- Goldstein, S.J., Murrell, M.T., Janecky, D.R., 1989. Th and U isotopic systematics of basalts from the Juan de Fuca and Gorda Ridges by mass spectrometry. *Earth and Planetary Science Letters* 96, 134–146.
- Harford, C.L., Sparks, R.S.J., 2001. Recent remobilization of shallow-level intrusions on Montserrat revealed by hydrogen isotope composition of amphiboles. *Earth and Planetary Science Letters* 185, 285–297.
- Heumann, A., Davies, G.R., Elliott, T., 2002. Crystallization history of rhyolites at Long Valley, California, inferred from combined U-series and Rb–Sr isotope systematics. *Geochimica et Cosmochimica Acta* 66, 1821–1837.
- Higgins, M.D., 1996. Magma dynamics beneath Kameni volcano, Thera, Greece, as revealed by crystal size and shape measurements. *Journal of Volcanology and Geothermal Research* 70, 37–48.
- Holness, M.B., Martin, V.M., Pyle, D.M., 2005. Information about open-system magma chambers derived from textures in magmatic enclaves: the Kameni Islands, Santorini, Greece. *Geological Magazine* 142, 637–649.
- Huijsmans, J.P.P., Barton, M., Salters, V.J.M., 1988. Geochemistry and evolution of the calc-alkaline volcanic complex of Santorini, Aegean Sea, Greece. *Journal of Volcanology and Geothermal Research* 34, 283–306.
- Jackson, M.D., Cheadle, M.J., Atherton, M.P., 2003. Quantitative modeling of granitic melt generation and segregation in the continental crust. *Journal of Geophysical Research* B7 (ECV3), 1–21.
- Keller, J., 1982. Mediterranean Island Arcs. In: Thorpe, R.S. (Ed.), *Andesites: Orogenic Andesites and Related Rocks*. Wiley, pp. 307–325.
- Martin, V.M., Holness, M.B., Pyle, D.M., 2006. Textural analysis of magmatic enclaves from the Kameni Islands, Santorini, Greece. *Journal of Volcanology and Geothermal Research* 154, 89–102.
- Mortazavi, M., Sparks, R.S.J., 2004. Origin of rhyolite and rhyodacite lavas and associated mafic inclusions of Cape Akrotiri, Santorini: the role of wet basalt in generating calcalkaline silicic magmas. *Contributions to Mineralogy and Petrology* 146, 397–413.
- Murphy, M.D., Sparks, R.S.J., Barclay, J., Carroll, M.R., Brewer, T.S., 2000. Remobilization of andesite magma by intrusion of mafic magma at the Soufriere Hills volcano, Montserrat, West Indies. *Journal of Petrology* 41, 21–42.
- Nicholls, I.A., 1971. Petrology of Santorini Volcano, Cyclades, Greece. *Journal of Petrology* 12 (1), 67–119.
- Peacock, M.A., 1931. Classification of igneous rock series. *Journal of Geology* 39, 54–67.
- Pe-Piper, G., Piper, D.J.W., 2002. *The Igneous Rocks of Greece: the Anatomy of an Orogen*. Gebrueder Borntraeger, Stuttgart. 573 pp.
- Petford, N., Cruden, A.R., McCaffrey, K.J.W., Vigneresse, J.L., 2000. Granite magma formation, transport and emplacement in the Earth's crust. *Nature* 408, 669–673.
- Pichavant, M., Martel, C., Bourdier, J.-L., Scaillet, B., 2002. Physical conditions, structure, and dynamics of a zoned magma chamber: Mount Pelée (Martinique, Lesser Antilles Arc). *Journal of Geophysical Research* 107 (ECV1), 1–28.
- Plank, T., Langmuir, C.H., 1998. The geochemical composition of subducting sediments and its consequence for the crust and mantle. *Chemical Geology* 145, 325–394.
- Potts, P.J., Thorpe, O.W., Isaacs, M.C., Wright, D.W., 1985. High precision neutron activation analysis of geological samples employing simultaneous counting with both planar and coaxial detectors. *Chemical Geology* 48, 145–155.
- Pyle, D.M., Ivanovich, M., Sparks, R.S.J., 1988. Magma cumulate mixing identified by U–Th disequilibrium dating. *Nature* 331, 157–159.
- Ramsey, M.H., Potts, P.J., Webb, P.C., Watson, J.S., Coles, B.J., 1995. An objective assessment of analytical method precision: comparison of ICP-AES and XRF for the analysis of silicate rocks. *Chemical Geology* 124, 1–19.
- Reagan, M.K., Sims, K.W.W., Erich, J., Thomas, R.B., Cheng, H., Edwards, R.L., Layne, G., Ball, L., 2003. Timescales of differentiation from mafic parents to rhyolite in North American continental arcs. *Journal of Petrology* 44, 1703–1726.
- Seymour, K.S., Lalonde, A.E., 1991. Monitoring oxygen fugacity conditions in pre-, syn- and postcaldera magma chamber of Nisyros volcano, Aegean island arc, Greece. *Journal of Volcanology and Geothermal Research* 46, 231–240.
- Seymour, K.S., Vlassopoulos, D., 1992. Magma mixing at Nisyros volcano, as inferred from incompatible trace-element systematics. *Journal of Volcanology and Geothermal Research* 50, 273–299.
- Smith, P.E., York, D., Chen, Y., Evensen, N.M., 1996. Single crystal ^{40}Ar – ^{39}Ar dating of a Late Quaternary paroxysm on Kos, Greece: concordance of terrestrial and marine ages. *Geophysical Research Letters* 23, 3047–3050.
- Sparks, R.S.J., Sigurdsson, H., Wilson, L., 1977. Magma mixing: a mechanism for triggering acid explosive eruptions. *Nature* 267, 315–318.
- Stamatopoulou-Seymour, K., Vlassopoulos, D., Pearce, T.H., Rice, C., 1990. The record of magma chamber processes in plagioclase phenocrysts at Thera Volcano, Aegean Volcanic Arc, Greece. *Contributions to Mineralogy and Petrology* 104, 73–84.
- Sun, S.S., McDonough, W.F., 1989. Chemical and isotopic systematics of oceanic basalts: implications for mantle composition and processes. In: Saunders, A.D., Norry, M.J. (Eds.), *Magmatism in Ocean Basins*. Geological Society Special Publications, pp. 313–345.
- Taylor, S.R., McLennan, S.M., 1995. The geochemical evolution of the continental crust. *Reviews of Geophysics* 33, 241–265.
- Tiepolo, M., Vannucci, R., Bottazzi, P., Oberti, R., Zanetti, A., Foley, S., 2000. Partitioning of rare earth elements, Y, Th, U, and Pb between pargasite, kaersutite, and basanite to trachyte melts:

- Implications for percolated and veined mantle. *Geochemistry, Geophysics and Geosystems* 1 2000GC000064.
- Turner, S., Hawkesworth, C., van Calsteren, P., Heath, E., Macdonald, R., Black, S., 1996. U-series isotopes and destructive plate margin magma genesis in the Lesser Antilles. *Earth and Planetary Science Letters* 142, 191–207.
- Turner, S., Evans, P., Hawkesworth, C., 2001. Ultrafast source-to-surface movement of melt at island arcs from ^{226}Ra – ^{230}Th systematics. *Science* 292, 1363–1366.
- Turner, S.P., Bourdon, B., Gill, J., 2003. Insights into magma genesis at convergent margins from U-series isotopes. In: Bourdon, B., Henderson, G.M., Lundstrom, C.C., Turner, S.P. (Eds.), *Uranium Series Geochemistry. Reviews in Mineralogy and Geochemistry. The Mineralogical Society of America, Washington*, pp. 255–315.
- van Calsteren, P., Schwieters, J.B., 1995. Performance of a thermal ionisation mass spectrometer with a deceleration lens system and post-deceleration detector selection. *International Journal of Mass Spectrometry and Ion Processes* 146/147, 119–129.
- Vanderkluyzen, L., Volentik, A.C.M., Principe, C., Hunziker, J.C., Hernandez, J., 2005. Nisyros' volcanic evolution: the growth of a stratovolcano. In: Hunziker, J.C., Marini, L. (Eds.), *The Geology, Geochemistry and Evolution of Nisyros Volcano (Greece). Implications for the Volcanic Hazards. Mémoires de Géologie, Lausanne*, pp. 100–106.
- Volentik, A.C.M., Vanderkluyzen, L., Principe, C., 2002. Stratigraphy of the Caldera walls of Nisyros volcano, Greece. *Eclogae Geologicae Helveticae* 95, 223–235.
- Volentik, A.C.M., Principe, C., Vanderkluyzen, L., Hunziker, J.C., 2005a. Geological Map of Nisyros Volcano (Greece). Chabloz Imprimerie, Lausanne.
- Volentik, A.C.M., Vanderkluyzen, L., Principe, C., Hunziker, J.C., 2005b. Stratigraphy of Nisyros Volcano (Greece). In: Hunziker, J. C., Marini, L. (Eds.), *The Geology, Geochemistry and Evolution of Nisyros Volcano (Greece). Implications for the Volcanic Hazards. Mémoires de Géologie, Lausanne*, pp. 26–66.
- Watson, E.B., Harrison, T.M., 1983. Zircon saturation revisited: temperature and composition effects in a variety of crustal magma types. *Earth and Planetary Science Letters* 64, 295–304.
- Wyers, G.P., Barton, M., 1989. Polybaric evolution of calc-alkaline magmas from Nisyros, Southeastern Hellenic Arc, Greece. *Journal of Petrology* 30, 1–37.
- Zellmer, G.F., Clavero, J., 2006. Using trace element correlation patterns to decipher a sanidine crystal growth chronology: an example from Taapaca volcano, Central Andes. *Journal of Volcanology and Geothermal Research* 156, 291–301.
- Zellmer, G.F., Turner, S.P., Hawkesworth, C.J., 2000. Timescales of destructive plate margin magmatism: new insights from Santorini, Aegean volcanic arc. *Earth and Planetary Science Letters* 174 (3–4), 265–282.
- Zellmer, G.F., Hawkesworth, C.J., Sparks, R.S.J., Thomas, L.E., Harford, C., Brewer, T.S., Loughlin, S., 2003a. Geochemical evolution of the Soufrière Hills volcano, Montserrat, Lesser Antilles Volcanic Arc. *Journal of Petrology* 44, 1349–1374.
- Zellmer, G.F., Sparks, R.S.J., Hawkesworth, C.J., Wiedenbeck, M., 2003b. Magma emplacement and remobilization timescales beneath Montserrat: insights from Sr and Ba zonation in plagioclase phenocrysts. *Journal of Petrology* 44, 1413–1431.
- Zellmer, G.F., Annen, C., Charlier, B.L.A., George, R.M.M., Turner, S.P., Hawkesworth, C.J., 2005. Magma evolution and ascent at volcanic arcs: constraining petrogenetic processes through rates and chronologies. *Journal of Volcanology and Geothermal Research* 140, 171–191.